

# Octave-spanning supercontinuum generation in highly nonlinear silica fibres based on cost-effective fibre amplifiers

J E Saldaña-Díaz<sup>1,2</sup> S Jarabo<sup>1</sup> and F J Salgado-Remacha<sup>1</sup>

<sup>1</sup> Universidad de Zaragoza, Departamento de Física Aplicada. Pedro Cerbuna 12, E-50009, Zaragoza, Spain.

<sup>2</sup> Universidad Nacional de Huancavelica, Departamento Académico de Ciencias Básicas, Facultad de Ciencias e Ingeniería, Huancavelica, Perú.

E-mail: fjsalgado@unizar.es

## Abstract

We report a simple method for supercontinuum generation. The set-up consists of an Er-doped mode-locked fibre laser, used as seed, and a highly nonlinear fibre with zero dispersion at 1550 nm. Thus, all the components are easily attainable. With this novel system the requirements in terms of control of dispersion are reduced. In addition, the spectral width is optimized using fibres with positive and negative dispersion. The supercontinuum emission is characterized by means of an Optical Spectrum Analyser and a PbS photodetector, showing an octave-spanning spectral width, with a flat profile from 1100 nm up to 2100 nm. Compared to other supercontinuum sources, this new proposal results in a very competitive and attainable system, particularly in the 1500-2100 nm region.

Keywords: Fibre lasers, Mode-locking, Nonlinear waveguides, Supercontinuum generation

PACS: 42.55.Wd, 42.60.Fc, 42.65.Wi

## 1. Introduction

Supercontinuum Generation (SCG) has been studied since decades ago [1] and demonstrated in a wide variety of nonlinear optical media, although these systems are usually complex, susceptible to vibrations, and require constant maintenance. However, fibre-based supercontinuum sources are simple, stable, compact and reliable. Moreover, they offer a broad spectrum spanning over several thousand of nanometres with a high spectral power density ( $> 1$  mW/nm) in near and medium infrared ranges. These sources usually employ Er and Er/Yb doped fibre pulsed lasers [2] to pump different types of fibres as nonlinear medium: photonic crystal fibres [3-6] generating up to 2.4  $\mu\text{m}$ , silica highly nonlinear fibres [7-13] up to 2.7  $\mu\text{m}$  and ZBLAN nonlinear fibres [14-16] up to 4.5  $\mu\text{m}$ . Other authors [17-19] have reported supercontinuum assisted by thulium-doped fibres generating powers from 2 to 2.5  $\mu\text{m}$ .

On the other hand, SCG in optical fibres is currently an active field of research due to the numerous applications such as optical coherence tomography, microscopy techniques, spectroscopic analysis of air and

water pollutants, optical communications or optical metrology in which supercontinuum sources are needed [15-16, 20-32].

Although the development of these sources is advanced enough, it is still necessary to improve their output spectral power and simplify the control of the dispersion in the nonlinear medium, since it involves nowadays some kind of difficulty in the design of SCG systems [33]. An alternative not much studied is based on the use of commercial optical amplifiers. In this way, the development of the pulsed laser and the amplification of the pulse that pumps the nonlinear fibre result easier. The spectral power of the supercontinuum would be improved as long as the pump pulse can be optimised by means of a suitable method.

In this manuscript we present a scheme of SCG source based on a mode-locking fibre laser for pumping and a highly nonlinear fibre (HNLf) as dispersive medium, where no control of dispersion is required. All the components, therefore, are common material in optics laboratories, reducing the costs and requirements for these systems. In addition, temporal and spectral characterization of the SCG source is provided, showing a spectrum covering from 1100 up to 2100 nm. The amplification needed for this system, moreover, results lower than the cited works. In this sense, we report an all-fibre feasible SCG source with competitive optical behaviour combined with an easily attainable and cost-effective set-up, compared with the current state of the art.

## 2. Experimental set-up

The scheme of the experimental set-up is shown in Fig. 1. A periodic train of ultrashort pulses source is generated by means of a passive mode-locked ring laser based on the nonlinear polarization rotation (NPR) effect. The laser cavity consists of an Erbium Doped Fibre Amplifier (EDFA) operating in the C-band (Highwave, model C20-G20-H-FC/APC-BTO 3.0, saturation output power of 20 dBm) as amplifier medium, an optical coupler extracting the 10% of the confined power, and an optical modulator based on the NPR effect, which is formed by a linear polarizer placed between two polarization controllers (General Photonics, model PLC-003-M-25). Output laser pulses are amplified by a second EDFA operating in the L-band (Keopsys, model KPS-BT2\_L-20-PB-FA, saturation output power of 20 dBm). A more complete description of this laser system can be found in Refs. [34-35].

In order to improve the peak power of the pulses and raise the nonlinear effects that originate supercontinuum emission, 111 m of a positive dispersion fibre (Corning, model SMF28e) are placed inside the laser cavity and 22 m of a negative dispersion fibre (Thorlabs, model DCF38) are added between the laser output and the second amplifier, as Fig. 1(a) shows. The optimal length of each fibre was determined by optimizing the second harmonic generation at 800 nm by means of a 2 mm length BBO crystal (Eksma Optics, model BBO-0608-16\*, type I, normal incidence). Moreover, the optimal length was also verified by means of supercontinuum spectrum observations.

This source is used as seed for supercontinuum generation in a HNLf (Yangtze Optical Fibre and Cable Company Ltd., NL-1550-Zero type). The nominal dispersion of this fibre at 1550 nm is null with a dispersion slope lower than  $0.025 \text{ ps nm}^{-2} \text{ Km}^{-1}$ . The nonlinear coefficient is over  $10 \text{ W}^{-1} \text{ Km}^{-1}$  and the Raman gain coefficient is higher than  $4.8 \text{ W}^{-1} \text{ Km}^{-1}$ .

The output power after the HNLf sample is the periodic train of pulses shown in Fig. 2, which has been measured by means of a fast photodiode (1 GHz bandwidth). The frequency of the pulses train is 1.39 MHz, which corresponds to a cavity of 148 meters.

( a )

EDFA-C

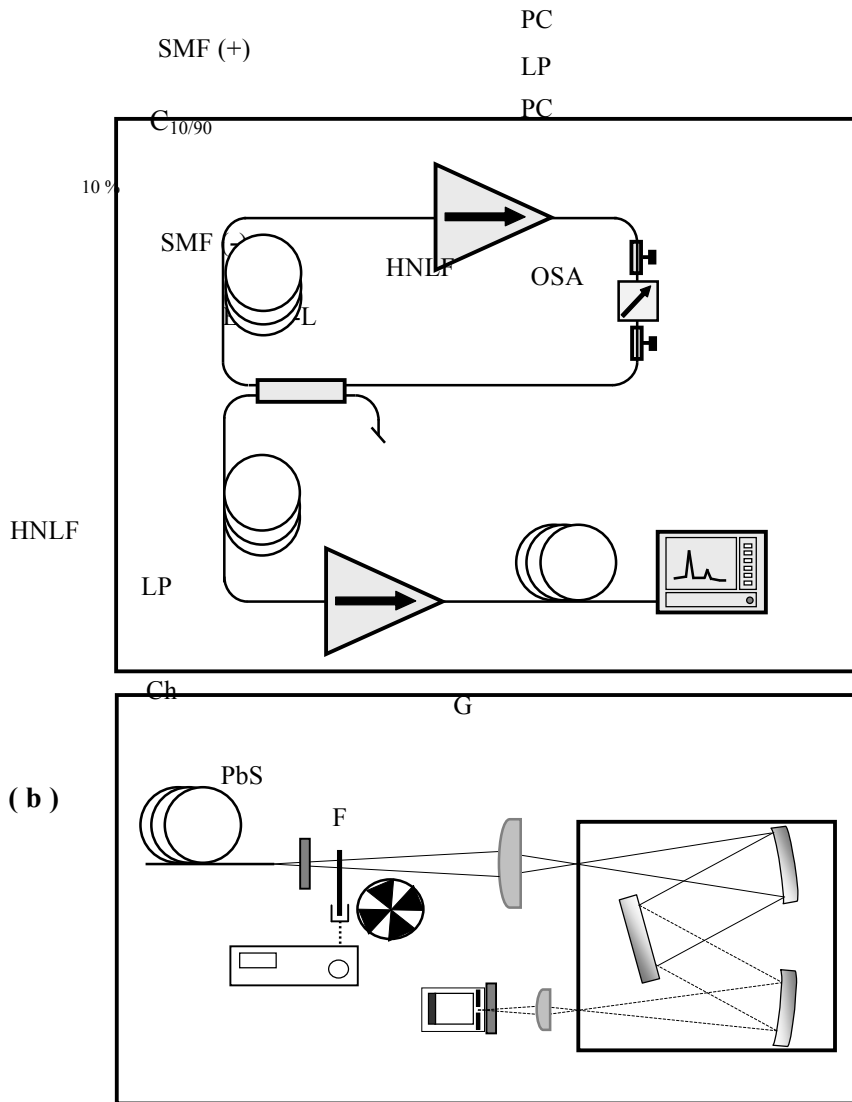


**Figure 1. Experimental set-up for supercontinuum generation in HNLf. (a) PC: polarization controller, LP: linear polarizer, C: coupler, EDFA-C: erbium-doped fibre amplifier in the C-band, EDFA-L: erbium-doped fibre amplifier in the L-band, SMF(+): single-mode fibre with positive dispersion, SMF(-): single-mode fibre with negative dispersion, HNLf: highly nonlinear silica fibre, OSA: optical spectrum analyser for spectral measurements up to 1700 nm; (b) the spectral range is extended up to 2550 nm by means of a monochromator and a PbS detector, Ch: chopper, F: longpass optical filter, G: grating.**

The optical spectrum up to 1700 nm is measured with a spectral resolution of 1 nm by means of an optical spectrum analyser (OSA, Agilent, model 86142B). The spectrum above 1700 nm is analysed with a spectral resolution of 4 nm by using a monochromator (SPEX, model 340E) with a diffraction grating with 300 grooves per millimetre and a Blaze wavelength of 2000 nm (Horiba Scientific) and is detected by means of a PbS photoconductor (spectral sensitivity from 1000 nm up to 2750 nm, Thorlabs, model FDPS3X3). In order to remove the influence of the second diffraction order, a longpass spectral filter (cut-on wavelength of 1500 nm, Thorlabs, model FEL1500) is placed in front of the photoconductor. A chopper together with a lock-in amplifier allows a synchronous detection. As the spectral efficiency of the diffraction grating depends on the polarization, a linear polarizer is added to the setup. Thus, the optical spectrum is measured for two orthogonal polarizations (vertical and horizontal). Both measurements are corrected using the calibration shown in Fig. 3. As can be seen, the spectral range of this set-up reaches up to 2550 nm.

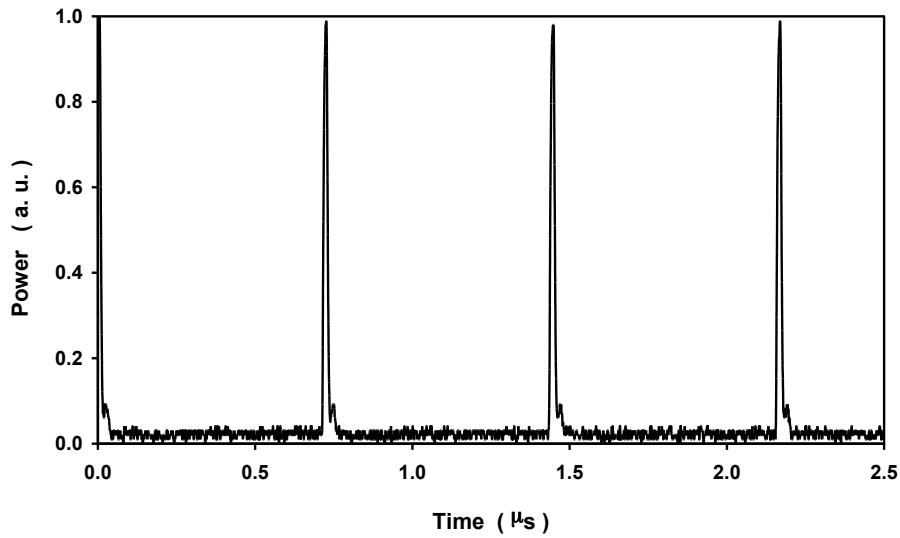


Figure 2. Pulses train (1.39 MHz) obtained after the HNLF.

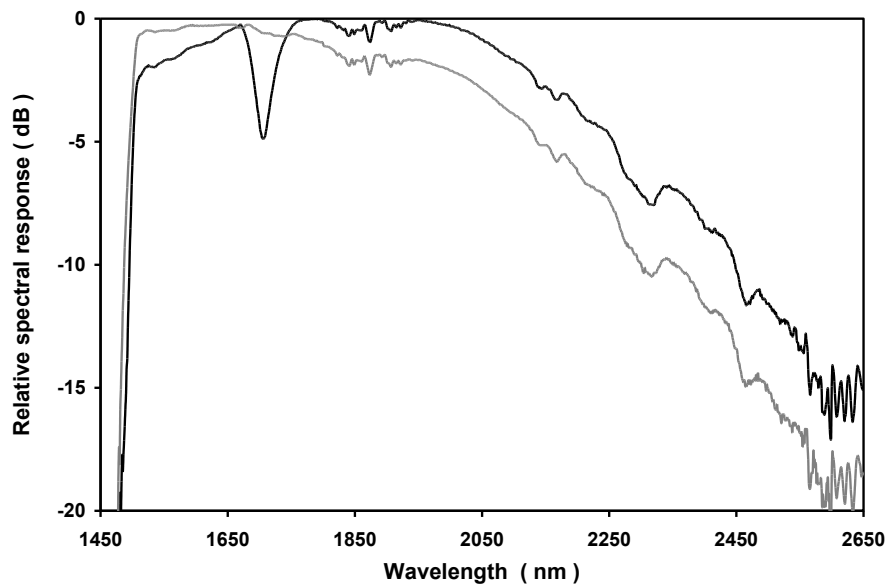


Figure 3. Relative spectral response of the experimental set-up for two orthogonal polarizations.

### 3. Supercontinuum Generation and optimization of the fibre lengths

In order to find the optimal length of HNLF for supercontinuum generation, we take spectra measurements with the set-up described in Section 2 for different HNLF lengths. Specifically, we have tested 10 m, 25 m, 63 m, 88 m, 102 m and 112 m. Fig. 4 gathers some of these measurements, showing that the best behaviour, in terms of spectral width, appear for a HNLF length of 63 m. In addition, the total spectral power for this length is bigger than in the other cases. We see that all the spectrum curves can be divided in three well-

differed parts; a flat spectral range from 1150 nm to 1480 nm, a depressed zone from 1480 nm to 1600 nm, and a second flat range from 1600 nm to 2200 nm, which has a higher spectral power.

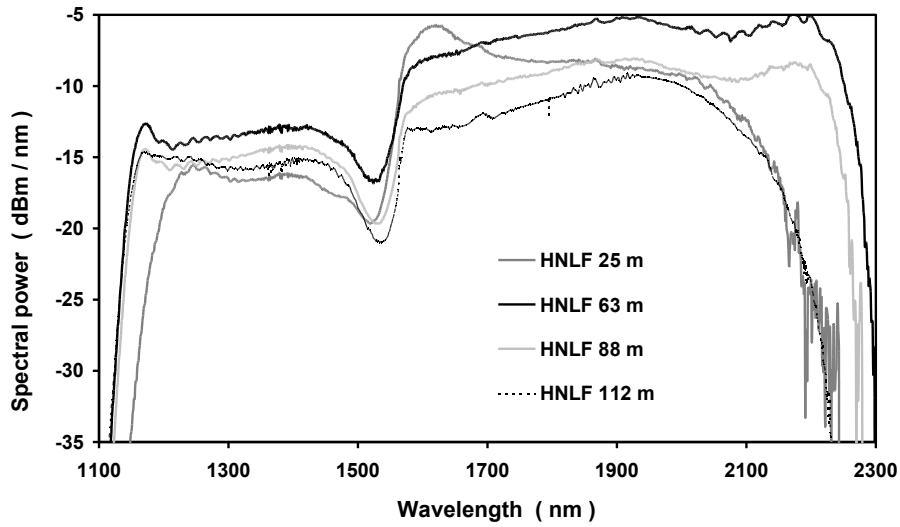


Figure 4. Supercontinuum spectra for different HNLF lengths, from 25 m up to 112 m. The maximum spectral width is found for 63 m.

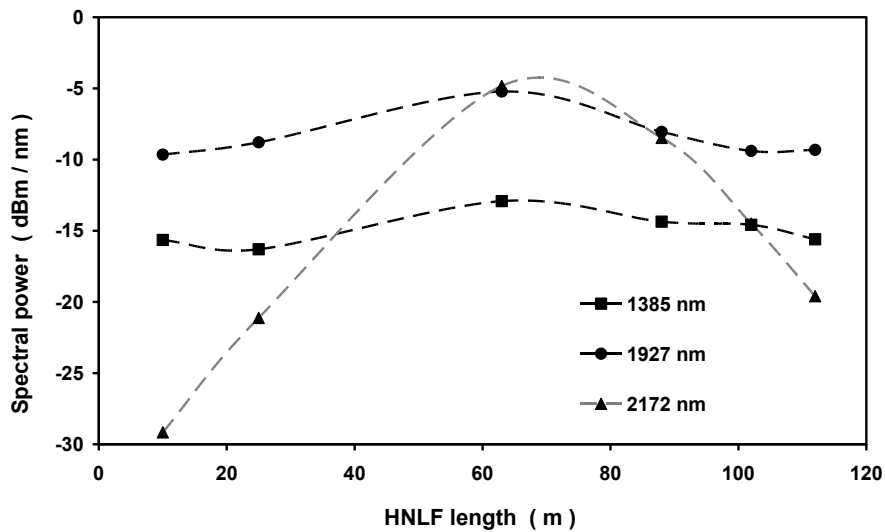


Figure 5. Spectral power at three different wavelengths (1385 nm, 1927 nm and 2172 nm) as a function of the HNLF length. Dotted curves are a visual aid only.

For a better understanding, Fig. 5 shows the spectral power at three different wavelengths, corresponding to 1385 nm (on the left side of the spectrum), 1927 nm (on the right side) and 2172 nm (at the border of the spectrum). We see that the maximum spectral power for each curve is reached when a HNLF length of 63 m is used. In addition, Fig. 6 collects the maximum and minimum wavelengths for each tested HNLF length,

taken at -20 dBm/nm. For clarity, Fig. 7 shows a more detailed curve of spectral width at -20 dBm/nm. It is clear that a length of 63 m produces a wider spectrum, reaching an octave. Thus, we will assume in the next sections that the optimal length is close to 63 m.

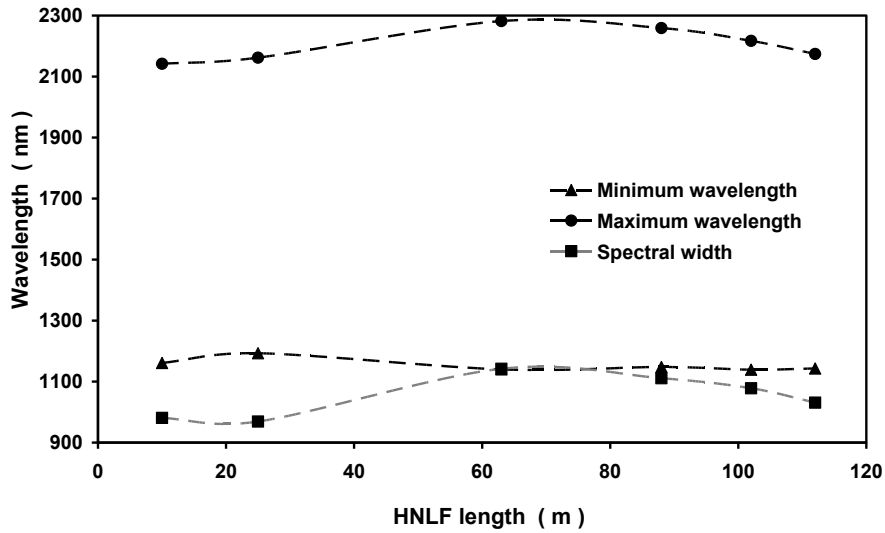


Figure 6. Maximum and minimum wavelengths and spectral width at -20 dBm/nm as a function of the HNLF length.

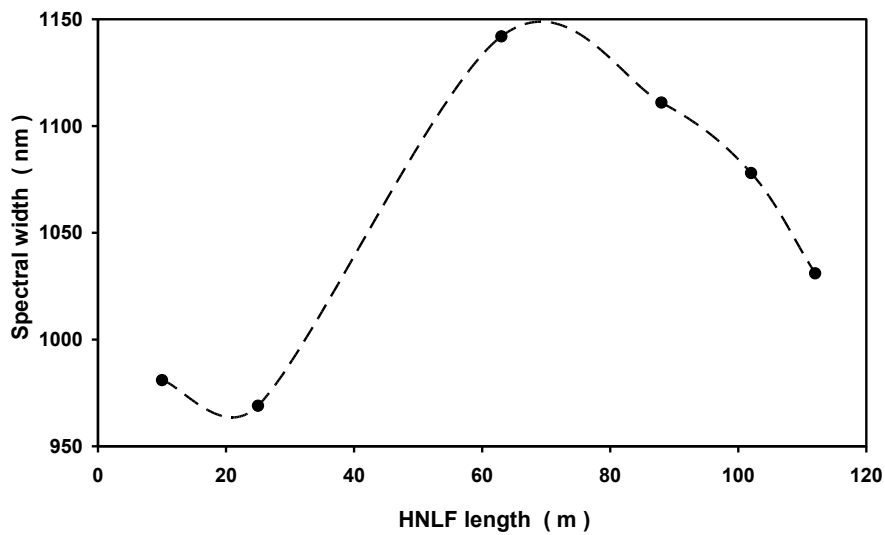


Figure 7. Spectral width at -20 dBm/nm as a function of the HNLF length. Dotted curves are a visual aid only.

It is clear that the supercontinuum spectrum has a lower limit around 1100 nm, and an upper limit in 2300 nm. Using a spectral filter (FB2750-500), we have corroborated that there is no emission from 2500 nm up to 3000 nm. At the same time, it is noticeable the origination of a spectral hole at 1523 nm (with a spectral power of -16.7 dBm/nm), dividing the spectrum in two sides. The right side of the spectrum (corresponding

to longer wavelengths) has more power, reaching up to -4.8 dBm. Table 1 summarizes the spectral details of the supercontinuum emission.

**Table 1. Spectral width of the supercontinuum emission generated with 63 m of HNLF ranges and spectral widths (in nm).**

| Minimum power (dBm/nm) | $\lambda_{\min}$ (nm) | $\lambda_{\max}$ (nm) | $\Delta\lambda$ (nm) |
|------------------------|-----------------------|-----------------------|----------------------|
| -17                    | 1147                  | 2278                  | 1131                 |
| <b>-20</b>             | <b>1140</b>           | <b>2282</b>           | <b>1142</b>          |
| -30                    | 1125                  | 2296                  | 1171                 |
| -40                    | 1112                  | 2299                  | 1187                 |

Thus, after the optimization process, we have found that the optimal HNLF length is 63 m. The optimized supercontinuum spectrum is shown in Fig. 8. We note the supercontinuum spectrum cover from 1140 nm up to 2282 nm over -20 dBm/nm, reaching an octave of spectral width. The upper limit of this spectrum matches with the common transmission limit of standard silica fibres.

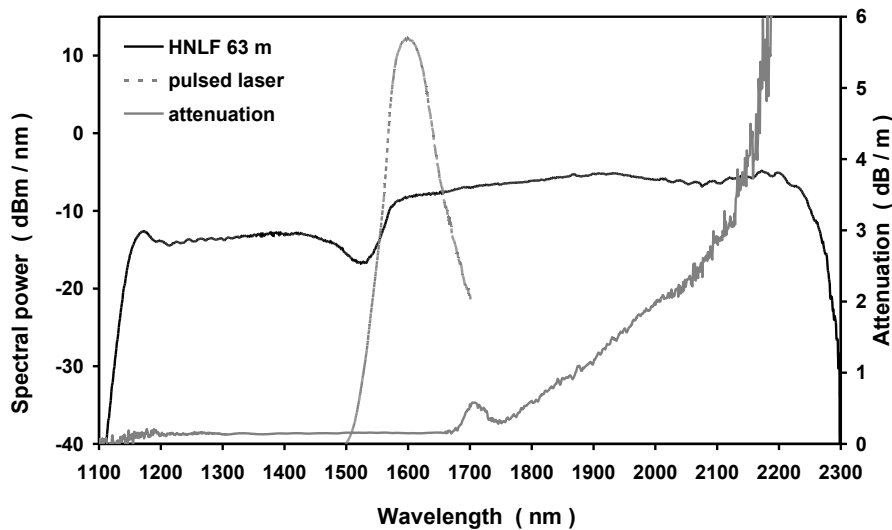


**Figure 8. Supercontinuum spectrum generated by 63 m of HNLF (solid line) and spectrum of the pulsed laser before HNLF, normal (dotted line), normalized to the unity.**

The use of positive (inside the cavity) and negative (between the pulsed laser and the second amplifier) dispersion fibres improves the spectrum of the supercontinuum emission. Specifically, playing with the dispersive fibres length it is possible to optimize the pulses features. However, the optimal dispersive fibres length does not depend on the HNLF length. Thus, Fig. 9 and Fig. 10 show this effect using 10 m and 102 m of HNLF, respectively. It is clear, in view of both figures, that a combination of these two dispersive fibres allows to enlarge slightly the spectrum width as well as increase the total power. Nevertheless, this

improvement is much more outstanding for short HNLF lengths. The proper lengths for these components results 111 meters for the positive dispersion fibres and 22 m for the negative dispersion fibre.

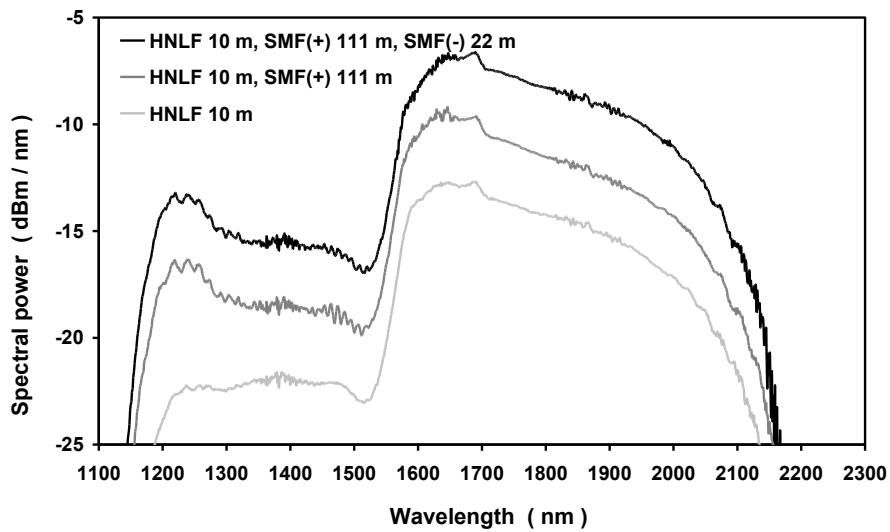


Figure 9. Improvement of the supercontinuum spectrum due to the use of positive and negative dispersion fibres, for 10 m of HNLF.

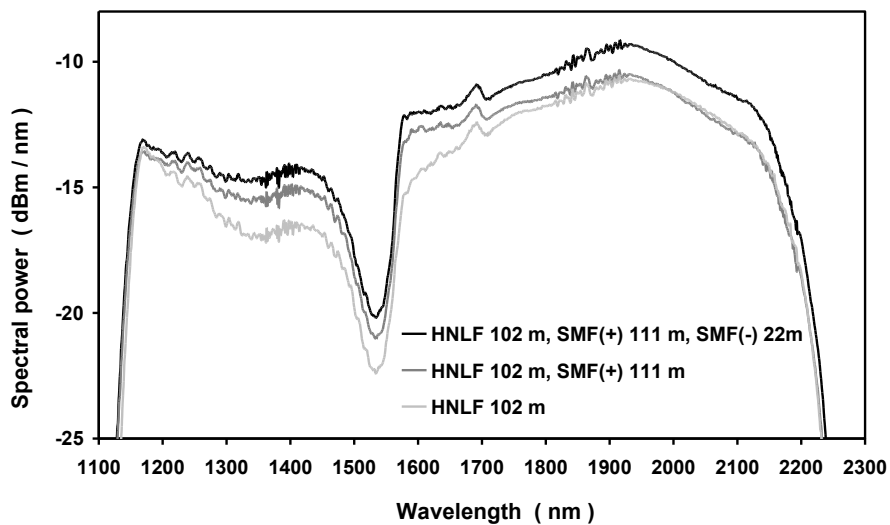


Figure 10. Improvement of the supercontinuum spectrum due to the use of positive and negative dispersion fibres, for 102 m of HNLF.

#### 4. Conclusions

We have reported in this work a novel set-up for supercontinuum generation. Compared with standard facilities, this new proposal stands out because of the simplicity and attainability. It is entirely based on commercial devices (like amplifiers) and silica fibres. For this reason, it can be easily implemented in common photonics laboratories. With the current version of the system, it is possible to reach an octave

spanning spectral width, which results very competitive compared to more complex set-ups (which commonly require more powerful amplification). Up to our knowledge, and excluding results based on ZBLAN fibres [14-16] or supercontinuum spectra with very low power, greater spectral widths in near-infrared range have only been reported in Refs. 12 and 31. Although different setups are compared in both references, only one of them obtains a wider spectrum, from 800 nm to 2400 nm, and only another of them offers longer wavelengths, up to 2500 nm, but beginning in 1500 nm. Moreover, a spectrum from 400 nm to 2200 nm by photonic crystal fibre is reported in Ref. 4. Nevertheless, due to the use of silica-based fibre, there exists an upper limit over 2000 nm. It could be possible in the future, however, to go beyond this limit increasing the amplification power in the system. This point opens the door to future works. The results in this work can be of interest for researches needing supercontinuum sources in the region of near-infrared. On the other hand, the spectral power obtained could be improved by means of two methods: by raising the pump power (the second amplifier should have a higher output power) or by shifting the pump wavelength to the zero-dispersion wavelength of the HNLF [15] (the second amplifier should operate in the C-band).

### Acknowledgements

This work was supported by the Ministerio de Economía y Competitividad (Programa Estatal de Fomento de la Investigación Científica y Técnica de Excelencia, project FIS2013-44174-P) and by the Diputación General de Aragón.

J E Saldaña acknowledges the financial support of Universidad de Zaragoza and Banco Santander (Doctoral Fellowship UZ-SANTANDER).

### References

- [1] Alfano R and Saphiro S 1970 Phys. Rev. Lett. **24** 584
- [2] Ouyang D Q, Guo G Y, Ruan S C, Yan P G, Wei H F and Luo J 2014 Laser Phys. **24** 045104
- [3] Jin A, Zhou H, Zhou X, Hou J, Jiang Z 2015 IEEE Photon. J. **7** 1600409
- [4] Gao S, Wang Y, Sun R, Li H, Tian C, Jin D and Wang P 2014 Opt. Express **22** 24697
- [5] Klimczak M, Siwicki B, Skibinski P, Pysz D, Stepien R, Heidt A, Radzewick C and Buczynski R 2014 Opt. Express **22** 18824
- [6] Labruyère A, Tonello A, Couderc V, Huss G, Leproux P 2012 Opt. Fiber Technol. **18** 375
- [7] Lin S S, Hwang S K and Liu J M 2014 Opt. Express **22** 4152
- [8] Rui S, Jing H, Ze-Feng W, Rui X and Qi-Sheng L 2013 Chin. Phys. B **22** 084206
- [9] Gao W, Liao M, Yan X, Suzuki T and Ohishi Y 2012 Appl. Opt. **51** 2346
- [10] Kamynin V A, Kurkov A S and Mashinsky V M 2012 Laser Phys. Lett. **9** 219
- [11] Swiderski J and Maciejewska M 2012 Appl. Phys. B **109** 177
- [12] Xia C, Kimar M, Cheng M Y, Kulkarni O P, Islam M N, Galvanauskas A, Terry F L, Freeman M J, Nolan D A and Wood W A 2007 IEEE J. Sel. Top. Quantum Electron. **13** 789
- [13] Nicholson J W, Yablon A D, Westbrook P S, Feder K S and Yan, M F 2004 Opt. Express **12** 3025

- [14] Heidt A. M., Price J. H. V., Baskiotis C., Feehan J. S., Li Z., Alam S. U., Richardson D. J., 2013 *Opt. Express* **21** 24281-7
- [15] Dupont S., Petersen C. Thogersen J., Agger C., Bang O., Keiding S. R., 2012, *Opt. Express* **20** 4887-92
- [16] Kumar M., Islam M. N., Terry F. L., Freeman M. J., Chan A., Neelakandan M., Manzur T., 2012 *App. Opt.* **51** 2794-2807
- [17] Dvoyrin V V and Sorokina I T 2014 *Laser Phys. Lett.* **11** 085108
- [18] Alexander V V, Shi Z, Islam M N, Ke K, Freeman M J, Ifarraguerra A, Meola J, Absi A, Leonard J, Zadnik J, Szalkowski A S and Boer G J 2013 *Opt. Lett.* **38** 2292
- [19] Yang W Q, Zhang B, Hou J, Xiao R, Song R and Liu Z J 2013 *Laser Phys. Lett.* **10** 045106
- [20] Shi L, Sordillo L A, Rodríguez-Contreras A and Alfano R 2016 *J. Biophotonics* **9** 38
- [21] Cheung C S, Daniel J M O, Tokurakawa M, Clarkson W A and Liang H 2015 *Opt. Express* **23** 1992
- [22] Gottschall T, Meyer T, Baumgartl M, Jáuregui C, Schmitt M, Popp J, Limpert J and Tunnermann A 2015 *Laser Photon. Rev.* **9** 435
- [23] Hattori Y, Kawagoe H, Ando Y, Yamanaka M and Nishizawa N 2015 *Appl. Phys. Express* **8** 082501
- [24] Pires H, Baudisch M, Sánchez D, Hemmer M and Biegert J 2015 *Prog. Quant. Electron.* **43** 1
- [25] Sordillo L A, Lindwasser L, Budansky Y, Leproux P and Alfano R 2015 *J. Biomed. Opt.* **20** 030501
- [26] Tsytkin A N, Putilin S E, Okishev A V and Kozlov S A 2015 *Opt. Eng.* **54** 056111
- [27] Werblinski T, Mittmann F, Altenhoff M, Seeger T, Zigan L and Will S 2015 *Appl. Phys. B* **118** 153
- [28] Kawagoe H, Ishida S, Aramaki M, Sakakibara Y, Omoda E, Kataura H and Nishizawa N 2014 *Biomed. Opt. Express* **5** 932
- [29] Korel I, Nyushkov B N, Denisov V I, Pivtsov V S, Koliada N A, Sysoliatin A A, Ignatovich S M, Kvashnin N L, Skvortsov M N and Bagayev S N 2014 *Laser Phys.* **24** 074012
- [30] Nishizawa N 2014 *Jpn. J. Appl. Phys.* **53** 090101
- [31] Swiderski J 2014 *Prog. Quant. Electron.* **38** 189
- [32] Medhurst L J 2005 *J. Chem. Educ.* **82** 278
- [33] Belal M, Xu L, Hoeak P, Shen I, Feng X, Ettabib M, Richardson D J, Petropoulos P and Price J H V 2015 *Opt. Lett.* **40** 2237
- [34] Lavieja C, Jarabo S, Marín-Doñágueda M and Sola Í J 2013 *Opt. Fiber Technol.* **19** 476
- [35] Jarabo S and Salgado-Remacha F J 2015 *Laser Phys. Lett.* **12** 095104